DR SORAYA PELAZ (Orcid ID : 0000-0001-7699-9330)

Article type : Original Article

TEMPRANILLO is a direct repressor of the microRNA miR172

Andrea E. Aguilar-Jaramillo[1], Esther Marín-González[1], Luis Matías-Hernández[1], Michela Osnato[1], Soraya Pelaz[1,2*] and Paula Suárez-López[1*]

[1] Centre for Research in Agricultural Genomics (CRAG), CSIC-IRTA-UAB-UB, Campus UAB, Bellaterra (Cerdanyola del Vallès), 08193 Barcelona, Spain; [2] Institució Catalana de Recerca i Estudis Avançats, 08010 Barcelona, Spain

* Authors for correspondence:
Soraya Pelaz
Tel: 34-93-5636600, ext. 3109
E-mail: soraya.pelaz@cragenomica.es

Paula Suárez-López
Tel: 34-93-5636600, ext. 3110
E-mail: paula.suarez@cragenomica.es,

Running title: TEMs regulate miR172

Keywords: Arabidopsis, flowering, juvenile-to-adult transition, miR172, SPL, TEMPRANILLO, vegetative phase change.

Summary

In the age-dependent pathway, the microRNA 156 (miR156) is essential for the correct timing of developmental transitions. MiR156 negatively regulates several *SPL* genes, which promote the juvenile-to-adult and floral transitions in part through up-regulation of miR172. The transcriptional repressors TEMPRANILLO1 (TEM1) and TEM2 delay flowering in *Arabidopsis thaliana* at least through direct repression of *FLOWERING LOCUS T* (*FT*) and

This article has been accepted for publication and undergone full peer review but has not been through the copyediting, typesetting, pagination and proofreading process, which may lead to differences between this version and the Version of Record. Please cite this article as doi: 10.1111/tpj.14455

gibberellins biosynthetic genes, and have also been reported to participate in the length of the juvenile phase. *TEM* mRNA and miR156 levels decrease gradually, allowing progression through developmental phases. Given these similarities, we hypothesized that TEMs and the miR156/SPL/miR172 module could act through a common genetic pathway.

We analyzed the effect of TEMs on miR156, *SPL* and miR172 levels, tested binding of TEMs to these genes using chromatin immunoprecipitation and analyzed the genetic interaction between *TEMs* and miR172. TEMs played a stronger role in the floral transition than in the juvenile-to-adult transition. TEM1 repressed *MIR172A*, *MIR172B* and *MIR172C* expressions and bound *in vivo* to at least *MIR172C* sequences. Genetic analyses indicated that TEMs affect the regulation of developmental timing through miR172.

INTRODUCTION

During their life cycle, plants go through several developmental transitions. The timing of these transitions is essential for proper development and adjustment of growth to environmental conditions. After germination, plants undergo a juvenile phase of vegetative growth, in which they are unable to flower, even under optimal environmental conditions. Following the juvenile period, there is a juvenile-to-adult transition, also termed vegetative phase change, leading to an adult phase in which plants become competent to flower (Huijser & Schmid, 2011). The juvenile-to-adult transition is associated with diverse morphological changes, and the appearance of trichomes on the abaxial side of rosette leaves is a conventional marker of this transition in *Arabidopsis thaliana* (Telfer *et al.*, 1997; Huijser & Schmid, 2011). In response to environmental and endogenous signals, adult plants experience a vegetative-to-reproductive or floral transition (Amasino, 2010; Andrés & Coupland, 2012).

Flowering is an energy-consuming process and therefore plants need to accumulate enough reserves before inducing the floral transition. To ensure that flowering occurs under favorable conditions, the transition to the reproductive phase is regulated by a complex genetic network that responds to environmental and endogenous cues (Amasino, 2010; Andrés & Coupland, 2012). Arabidopsis flowers earlier under long day (LD) than short day (SD) conditions. We have previously shown that *TEMPRANILLO 1* (*TEM1*) and *TEM2* (also known as *RAV2*) inhibit flowering at early developmental stages under LDs and SDs (Castillejo & Pelaz, 2008; Osnato *et al.*, 2012). TEMs belong to the RAV subfamily of transcription factors (Matías-

Hernández *et al.*, 2014), which bind DNA at the consensus sequence C(A/C/G)ACA$(N)_{2-8}$(C/A/T)ACCTG (Kagaya *et al.*, 1999). TEMs delay flowering through direct transcriptional repression of genes encoding the florigen component FLOWERING LOCUS T (FT), its paralog TWIN SISTER OF FT (TSF), and the gibberellin (GA) biosynthesis enzymes GIBBERELLIN 3-OXIDASE 1 (GA3OX1) and GA3OX2 (Castillejo & Pelaz, 2008; Osnato *et al.*, 2012; Marín-González *et al.*, 2015). Thus, in Arabidopsis, RAV proteins act as transcriptional repressors (Castillejo & Pelaz, 2008; Ikeda & Ohme-Takagi, 2009; Causier *et al.*, 2012; Osnato *et al.*, 2012; Feng *et al.*, 2014; Marín-González *et al.*, 2015). Recently, a role for TEMs in the control of juvenility in Arabidopsis has been reported (Sgamma *et al.*, 2014). Therefore, TEMs play a role in two aspects of developmental timing, the juvenile-to-adult and the floral transitions.

Among the small RNAs involved in the regulation of plant developmental timing, the microRNAs (miRNAs) miR156 and miR172 play a very prominent role (Poethig, 2009; Rubio-Somoza & Weigel, 2011). In diverse plant species, miR156 delays vegetative phase change and flowering through downregulation of several *SQUAMOSA PROMOTER BINDING PROTEIN-LIKE* (*SPL*) genes (Wang & Wang, 2015). In Arabidopsis, these miR156 target genes include *SPL3*, *SPL4*, *SPL5*, *SPL9*, *SPL10* and *SPL15* (Wu & Poethig, 2006; Gandikota *et al.*, 2007; Schwarz *et al.*, 2008; Wu *et al.*, 2009; Hyun *et al.*, 2016). Plants overexpressing miR156 (*35S::miR156*) show a delayed juvenile-to-adult transition, flower late and have reduced *SPL* mRNA levels (Schwab *et al.*, 2005; Wu & Poethig, 2006; Gandikota *et al.*, 2007; Wang *et al.*, 2009; Wu *et al.*, 2009). Conversely, plants in which miR156 function is reduced (*35S::MIM156* plants) lack the juvenile phase, flower early and have increased *SPL* mRNA levels (Franco-Zorrilla *et al.*, 2007; Wang *et al.*, 2009; Wu *et al.*, 2009).

Although single mutants of the miR156-targeted *SPL* genes show very weak or no obvious phenotypes under LDs, double *spl9 spl15* mutants show delayed juvenile-to-adult and floral transitions, revealing functional redundancy within the *SPL* family (Wu & Poethig, 2006; Schwarz *et al.*, 2008; Wang *et al.*, 2008). The function of the miR156/SPL module has also been investigated using miR156-resistant versions of *SPL* genes (*rSPL*). Plants overexpressing *rSPL3*, *rSPL4* or *rSPL5* show early vegetative phase change and early flowering and plants expressing *rSPL9* or *rSPL15* under the control of their own promoters

show even stronger phenotypes (Wu & Poethig, 2006; Gandikota *et al.*, 2007; Wu *et al.*, 2009; Hyun *et al.*, 2016).

MiR156 and miR172 show opposite temporal expression patterns, such that miR156 decreases and miR172 increases with age (Aukerman & Sakai, 2003; Wu & Poethig, 2006; Jung *et al.*, 2007; Wang *et al.*, 2009; Wu *et al.*, 2009). MiR156 represses miR172 expression via down-regulation of SPL9 and SPL15, which promote miR172 expression (Wu *et al.*, 2009; Hyun *et al.*, 2016). In turn, miR172 promotes the juvenile-to-adult and the floral transitions, given that miR172 overexpression accelerates these transitions and reduced miR172 function delays flowering (Aukerman & Sakai, 2003; Chen, 2004; Wu *et al.*, 2009; Todesco *et al.*, 2010; Jung *et al.*, 2011). MiR172 down-regulates its target genes, which encode six APETALA2 family transcription factors (Aukerman & Sakai, 2003; Chen, 2004). All six redundantly repress flowering and at least three of them delay the juvenile-to-adult transition (Aukerman & Sakai, 2003; Chen, 2004; Jung *et al.*, 2007; Mathieu *et al.*, 2009; Wu *et al.*, 2009; Yant *et al.*, 2010; Jung *et al.*, 2011). Therefore, miR156, SPLs, miR172 and the miR172 target genes constitute an age-dependent developmental pathway, in which complex feedback regulations have been reported (Schwab *et al.*, 2005; Mathieu *et al.*, 2009; Wu *et al.*, 2009; Yant *et al.*, 2010; Jung *et al.*, 2011).

Similar to miR156, *TEM1* and *TEM2* mRNA levels decline with age (Castillejo & Pelaz, 2008) and have been reported to participate in juvenility length (Sgamma et al., 2014). Given the similar expression patterns and similar phenotypic effects of TEMs and miR156 on vegetative phase change and flowering, we hypothesized that TEMs and the miR156/SPL/miR172 module may act through a common genetic pathway. We show here that TEMs negatively regulate miR172 levels. TEM1 binds to *MIR172C* chromatin and directly regulates its expression, and also regulates that of *MIR172A* and *MIR172B*. In addition, miR172 partially mediates the effects of TEMs on vegetative phase change and flowering. Therefore, we conclude that TEMs regulate developmental timing in part through this miRNA involved in the age-dependent pathway.

RESULTS

Comparison of phenotypes caused by alterations in TEM1/TEM2 and the age-dependent pathway

In order to uncover the mechanism of TEM1/TEM2 action on phase change, we compared the phenotypes of plants with altered *TEM* levels with those of plants affected in the age-dependent pathway under SDs and LDs. It has been shown that miR156 maintains the juvenile traits by repressing SPLs, that in turn activate miR172 which will promote adult epidermal identity, such as the appearance of trichomes on the abaxial surface of rosette leaves (Poethig 2003, 2013, Huijser and Schmid, 2011, Yu et al., 2015; Wang et al., 2019). The timing of abaxial trichome formation is correlated with flowering time, consistent with the fact that juvenile-to-adult vegetative phase change contributes to the acquisition of the competence to flower. Thus, miR172 is involved in the timing of trichome formation, and its AP2 target genes, together with KANADI, have been shown to mediate the temporal and spatial integration for abaxial trichome formation (Wang et al., 2019). Interestingly, alterations of *TARGET OF EAT 1* (*TOE1)* or miR172 levels affect the timing of abaxial, but not adaxial, trichome formation (Wang et al., 2019). Consequently, the length of juvenile or adult phases can be determined by counting the leaves without and with abaxial trichomes, respectively.

Under SDs, we confirmed previously reported results and used them as control for our *tem* mutant plants growing in parallel. Thus, *35S::miR156* plants showed a dramatically extended juvenile phase, consistent with the results of Wu *et al*. (2009), and a shortened adult phase (Figures 1a,b, S1a,b; Table S2a,b), resulting in late flowering compared with wild-type plants (Figures 2a,b, S2a,b; Table S3a,b). Plants in which miR156 activity was inhibited (*35S::MIM156*) and plants expressing a miR156-resistant form of SPL9 (*pSLP9::rSPL9*) lacked the juvenile phase, in agreement with a previous report (Wu *et al.*, 2009), and had an adult phase similar to that of wild-type plants under SDs (Figures 1a,b, S1a-d; Table S2a,b). Therefore, *35S::MIM156* and *pSLP9::rSPL9* plants flowered with fewer leaves than wild-type plants (Figures 2a, S2a,c; Table S3a) due to the absence of the juvenile phase. *35S::MIM172* plants showed longer juvenile and adult phases than wild-type plants (Table S2a,b), and flowered with statistically significant more leaves than wild-type plants (Figures 2a, S2c; Table S3a), consistent with previous reports (Todesco *et al.*, 2010; Galvão *et al.*, 2012).

Under SDs the length of the juvenile phase of *tem1* and *tem2* single mutants was not altered, whereas *tem1 tem2* double mutants displayed a slightly shorter juvenile phase than the wild type (Figures 1a,c, S1a,e; Table S2a,c), indicating that TEM1 and TEM2 delay the juvenile-to-adult transition in a redundant manner. *tem2* and *tem1 tem2* mutants had a significantly shorter adult phase than wild-type plants (Figures 1b,d, S1b,f; Table S2b,d). Consistent with a shortened adult phase and with previous reports (Castillejo & Pelaz, 2008; Osnato *et al.*, 2012), early flowering was observed in *tem1*, *tem2* and, more markedly, in *tem1 tem2* (Figures 2a-d, S2a,b,e,f; Table S3a-d). Plants overexpressing *TEM1* (*35S::TEM1*) had a dramatically extended juvenile phase (>113 juvenile leaves) and neither transitioned to the adult phase nor flowered for at least 4 months under SDs. Overall, similar results were obtained under LDs (Figures 1e-j, 2e-j, S1g-l, S2g-l; Tables S2e-j, S3e-j). Under this condition, *35S::TEM1* plants also showed a substantially long juvenile phase, an unexpectedly short adult phase (Figures 1i,j, S1k,l; Table S2i,j) and flowered later than the wild-type (Figures 2i,j, S2k,l; Table S3i,j). Most *35S::TEM1* plants did not produce leaves with abaxial trichomes, probably due to the fact that these plants, in addition to having a late juvenile-to-adult transition, produce very few leaf trichomes (Matías-Hernández *et al.*, 2016). Due to the similar results obtained with all genotypes under both photoperiods we therefore used LD conditions for all subsequent experiments.

Because of the lack of other *tem1* and *tem2* alleles, we analyzed the length of the juvenile and adult phases of *RNAi-TEM1/2* plants, in which both *TEM1* and *TEM2* are partially silenced (Castillejo & Pelaz, 2008) to confirm the effect of TEMs on the juvenile-to-adult transition. Consistent with the results obtained in *tem1 tem2* mutants, *RNAi-TEM1/2* plants exhibited shorter juvenile and adult phases than wild-type plants under LDs (Figures 3, S3; Table S4a,b). *RNAi-TEM1/2* also flowered earlier than the wild type under this condition (Figures 4, S4; Table S5a,b), in agreement with previous results (Castillejo & Pelaz, 2008).

We can conclude that TEMs and the miR156/SPL module affect the juvenile-to-adult and floral transitions to different extents, with the miR156/SPL module having a more dramatic effect on the juvenile phase and TEMs affecting more strongly the floral transition, with a much smaller effect on the regulation of vegetative phase change. Therefore, our results suggest that the miR156/SPL module and TEM1/TEM2 play partially overlapping but distinct roles in the regulation of phase transitions.

TEMs do not act through *MIR156* or *SPL* genes

TEMs and miR156 affect the juvenile-to-adult and the floral transitions under both LDs and SDs (Figures 1-4, S1-S4; Schwab *et al.*, 2005; Wu & Poethig, 2006; Franco-Zorrilla *et al.*, 2007; Castillejo & Pelaz, 2008; Wu *et al.*, 2009; Osnato *et al.*, 2012; Sgamma et al., 2014). As miR156 and TEM1/TEM2 follow similar temporal expression patterns and have partially overlapping phenotypic effects, we tested whether miR156 regulates *TEM1*/*TEM2* levels or vice versa. *35S::miR156* and *35S::MIM156* plants did not show significant alterations in *TEM1* and *TEM2* mRNA levels that could correlate with their flowering phenotypes under LD and SD conditions (Figure S5). For the analysis of the effect of TEMs on miR156, we collected samples at two time points under LD, one during the light period (ZT8), when *TEM* mRNA levels are low (Castillejo & Pelaz, 2008; Osnato *et al.*, 2012) and the miR156-targeted *SPL9* mRNA peaks (Figure S6), and one during the night (ZT18), when *TEM* mRNAs peak (Castillejo & Pelaz, 2008; Osnato *et al.*, 2012). Although RNA blots with samples collected at one time point, ZT8 in 10-day-old plants, showed slight differences (Figure S7a,b), when we examined miR156 levels in *tem1 tem2* mutants at different ages, we did not observe substantial differences relative to wild-type plants (Figure S7c). Even the miR156 level reduction happened at the same time, after day 12, in both genotypes and, therefore, we could not confirm that TEMs have an effect on miR156 (Figure S7c).

Then we tested the effect of TEMs on the expression of *SPL* genes under LDs. As previously, when we studied *SPL3*, *SPL9* and *SPL15* expressions at one time point we found that *SPL3* transcript abundance was slightly increased in 10-day-old *tem1 tem2* plants (Figure 5a-c) and that the expression of all three genes was reduced in *35S::TEM1* plants (Figure 5a-c), but an analysis of *SPL* mRNA levels at different ages confirmed that only *SPL3* and *SPL9* were down-regulated in *35S::TEM1* plants (Figure 5d-i) and none was affected in *tem1 tem2* mutant plants (Figure 5d-i).

TEMs down-regulate miR172 and bind to *MIR172C* chromatin

Since TEMs were reported to have a role in the length of the juvenile phase (Sgamma et al., 2014) and we have not observed expression changes of miR156 or *SPL* genes in *tem1 tem2* mutant plants, we wondered if the effect on the phase transition could be through miR172 whose genes transcription is activated by SPLs (Wu et al., 2009). Consistent with this hypothesis, we found increased abundance of mature miR172 in *tem1 tem2* and reduced abundance in *35S::TEM1* when we analyzed 10-day-old plants (Figure 6a,b). Similar results

were obtained by RNA blot (Figure 6a,b) and RT-qPCR (Figure S8). *35S::miR156* and *pSPL9::rSPL9* plants used as controls showed slightly reduced and increased miR172 levels, respectively (Figure 6a), as expected (Wu *et al.*, 2009). Then we examined mature miR172 levels in *tem1 tem2* mutants at different ages. Again, we found that *tem1 tem2* mutants show increased miR172 levels up to day 12 (Figure 6c), indicating that TEMs down-regulate miR172 at early developmental stages, consistent with their effect on the juvenile-to-adult and floral transitions.

We found putative RAV binding sites in four *MIR172* genes (Table S6). We chose *MIR172C* gene because it has several putative RAV binding sites and it was possible to design specific oligos to test binding of TEM1 and TEM2 by ChIP. TEM1 clearly bound to a fragment containing two putative RAV binding sites and TEM2 also bound to some extent (Figure 6d). This suggests that TEMs repress miR172 expression through direct binding to, at least, *MIR172C* chromatin. We used transient expression assays in Arabidopsis protoplasts to test whether this is the case. Indeed, we found that TEM1 represses expression of a reporter construct that carries a fragment of the *MIR172C* gene containing the two RAV binding sites bound in ChIP experiments (Figure 6e). In addition, *MIR172C* transcript levels are increased in *tem1 tem2* and *RNAi-TEM1/2* plants, and are decreased in *35S::TEM1* plants (Figure 6f). Similarly, we found that *MIR172A* and *MIR172B* transcript levels are increased when *TEM* genes are down-regulated and that *MIR172A* levels are decreased when *TEM1* is overexpressed (Figure 6f). Upregulation of the three *MIR172A*, *MIR172B* and *MIR172C* genes resulted in the high mature miR172 levels observed in *tem1 tem2* mutant plants (Figure 6a,c and S8). TEMs, therefore, down-regulate miR172 levels by binding to at least the *MIR172C* gene and repressing its transcription.

TEMs act partially through miR172

If the early vegetative phase change and early flowering of *tem1 tem2* and *RNAi-TEM1/2* plants is due to increased miR172 abundance, silencing of miR172 should suppress the vegetative phase change and flowering phenotypes of *tem1 tem2* and *RNAi-TEM1/2*. Unfortunately, we found that several transgenes were silenced when introduced in *tem1* and *35S:TEM1* mutant backgrounds (Figure S9a,b,c). Silencing of transgenes by T-DNA insertion mutations has already been reported (e.g. Daxinger *et al.*, 2008; Wu *et al.*, 2009). Therefore, to analyze the genetic interaction between *TEMs* and miR172 we crossed *35S::MIM172* with *RNAi-TEM1/2* and checked that the *35S::MIM172* transgene was not

silenced (Figure S10). If miR172 acts downstream of TEM1 to control vegetative phase change and flowering, we would expect that inactivation of miR172 would suppress the phenotypes of *RNAi-TEM1/2* plants. Our results showed that *35S::MIM172* plants had longer juvenile and adult phases and flowered later and after producing more leaves than WT plants (Figures 7, 8, S11, S12; Tables S7a,b, S8a,b). *RNAi-TEM1/2 35S::MIM172* plants had intermediate phenotypes between *35S::MIM172* and *RNAi-TEM1/2*: they had longer juvenile and adult phases than *RNAi-TEM1/2* plants, but had shorter phases than *35S::MIM172* plants (Figures 7, S11; Table S7a,b), and they flowered with more leaves than *RNAi-TEM1/2*, but with fewer leaves than *35S::MIM172* plants (Figures 8, S12; Table S8a). These results indicate that *35S::MIM172* suppresses partially the early juvenile-to-adult transition and the early flowering of *RNAi-TEM1/2*. Taking together these results and the effect of TEMs on miR172 levels, we can conclude that TEMs delay flowering, and to a lesser extent the vegetative phase change, partially through miR172.

DISCUSSION

TEMs regulate miR172 levels

Several flowering-time regulators, such as FCA, GIGANTEA, SHORT VEGETATIVE PHASE, SUPPRESSOR OF OVEREXPRESSION OF CO 1, SPL9, and SPL15, affect miR172 levels. Several of these genes regulate transcription of *MIR172* genes, whereas others affect processing of miR172 primary transcripts (Jung *et al.*, 2007; Wu *et al.*, 2009; Lee *et al.*, 2010; Cho *et al.*, 2012; Jung *et al.*, 2012b; Tao *et al.*, 2012; Hyun *et al.*, 2016). In addition, proteins of the POLYCOMB REPRESSIVE COMPLEX 1 (PRC1) and PRC2, which establish and maintain transcriptional repression through histone modifications, repress *MIR172B* expression (Picó *et al.*, 2015). Our work establishes that TEMs are new miR172 regulators (Figure 6). Whereas all the previously reported miR172 regulators have been shown to affect expression or processing of *MIR172A* and/or *MIR172B*, we show here that TEMs regulate *MIR172A*, *MIR172B* and *MIR172C* expressions. Therefore, multiple flowering-time regulators fine-tune mature miR172 levels by regulating several *MIR172* genes. Further work will be required to understand whether there are interactions among all these factors and how they contribute to establish the temporal and spatial pattern of miR172 expression.

TEM1 and TEM2 had been described as transcriptional repressors that directly down-regulate *FT*, *TSF*, *GA3ox1* and *GA3ox2* (Castillejo & Pelaz, 2008; Osnato *et al.*, 2012; Marín-González *et al.*, 2015). We show here that TEMs down-regulate miR172 levels through direct binding to at least one *MIR172* gene, *MIR172C*, and transcriptional repression of *MIR172A*, *MIR172B* and *MIR172C* (Figure 6). Although the molecular mechanism of this repression has yet to be elucidated, TEM1 and TEM2 interact with the transcriptional corepressor TOPLESS (Causier *et al.*, 2012), which forms a complex with and requires the activity of histone deacetylases (Long *et al.*, 2006; Krogan *et al.*, 2012; Wang *et al.*, 2013). It is possible, then, that TEMs repress transcription by recruiting histone modification factors through their interaction with TOPLESS, or that these interactions contribute to maintenance of transcriptional repression.

Our work and that of other groups suggests that TEMs can repress SPL expression (Figure 5) and function through several mechanisms. Given that FT and GAs are positive regulators of several *SPL* genes (Yamaguchi *et al.*, 2009; Galvão *et al.*, 2012; Jung *et al.*, 2012a; Park *et al.*, 2013), the repression of *FT* expression and GA biosynthesis by TEMs (Castillejo & Pelaz, 2008; Osnato *et al.*, 2012) may lead to indirect transcriptional down-regulation of *SPLs*. TEMs can also exert post-translational regulation of SPLs through the repression of GA biosynthesis (Osnato *et al.*, 2012), as DELLA proteins interfere with SPL transcriptional activity through direct interaction, and GA releases this interaction (Yu *et al.*, 2012). We hypothesize that TEMs can also indirectly repress *SPL* expression through feedback loops mediated by miR172 target genes. There is feedback regulation of *SPL* genes by miR172 target genes, such that miR172 target genes negatively regulate several *SPLs* or positively regulate miR156 (Yant *et al.*, 2010; Jung *et al.*, 2011). This indirect feedback on miR156 might result in the observed differential effect on *SPL* expressions, as *SPL3* transcript has recently been shown to be more sensitive to miR156 cleavage than *SPL9* or *SPL15* (He et al., 2018). It is possible, therefore, that the down-regulation of *SPL3* and *SPL9* observed in *35S::TEM1* plants (Figure 5a-i) is an indirect consequence of the downregulation of miR172 (Figure 6b) – and the expected up-regulation of miR172 targets - in these plants. All this would contribute to ensure that SPLs do not promote precocious juvenile-to-adult transition and flowering.

The regulation of flowering by TEMs is partially mediated by miR172

The flowering phenotypes of *tem1 tem2* double mutants and *RNAi-TEM1/2* plants are stronger than those of *tem1* and *tem2* single mutants (Figures 2, 4; Castillejo & Pelaz, 2008; Osnato *et al.*, 2012), indicating that both TEM1 and TEM2 are required for delaying flowering. Our work shows that the early flowering phenotype of *RNAi-TEM1/2* plants is partially suppressed by the inactivation of miR172 function in *RNAi-TEM1/2 35S::MIM172* plants (Figure 8). Together with the binding of TEMs to *MIR172C* chromatin, the effect of TEMs on *MIR172A*, *MIR172B* and *MIR172C* RNAs and mature miR172 levels (Figure 6), indicates that TEMs regulate flowering partly through miR172, by repressing the expression of *MIR172A*, *MIR172B* and directly that of *MIR172C*. Taking into account previous reports, we can conclude that the regulation of flowering time by TEMs is mainly mediated by FT, TSF and gibberellin (Castillejo & Pelaz, 2008; Osnato *et al.*, 2012; Marín-González *et al.*, 2015), but also partially by miR172.

TEMs play a more modest role in the juvenile-to-adult transition

We had previously shown that TEM1 and TEM2 play a role in the timing of the floral transition in Arabidopsis (Castillejo & Pelaz, 2008; Osnato *et al.*, 2012). We show here that they also somewhat affect the timing of vegetative phase change. In a previous work, it was showed a more dramatic effect of TEMs on the juvenile phase (Sgamma *et al.*, 2014). However, they determined the length of the juvenile phase by the response of flowering to inductive photoperiods and measured number of days from germination, whereas we measured the number of leaves without abaxial trichomes (Telfer *et al.*, 1997; Huijser & Schmid, 2011; Wang et al., 2019). In addition, we cannot rule out that the difference can be due to the use of different growth conditions. Taking into account that determining the juvenile phase length by measuring the competence to flower after LD exposure may not be the same as determining it by counting the number juvenile leaves, our results (Figure 1 and 3), although with a much weaker effect, seem consistent with those of Sgamma *et al.* (2014) as we both observed that TEM1 and TEM2 redundantly delay vegetative phase change.

Unexpectedly, when *TEM1* is overexpressed, instead of an extension of the adult phase, we observed a dramatic lengthening of the juvenile phase under both LDs and SDs, together with an extreme shortening or even suppression of the adult phase under LDs (Figure 1i,j). However, *35S::TEM1* plants show a dramatically reduced trichome density (Matías-Hernández *et al.*, 2016). Therefore, it is possible that the alteration of the number of leaves

without and with abaxial trichomes in these plants is a combination of the effects on the juvenile-to-adult transition and on trichome density.

The different genetic pathways acting in the flowering time network share several genes (Bouché *et al.*, 2016). By revealing the role of TEMs in the age-dependent flowering pathway, our work suggests that TEMs link this pathway to the photoperiod, GA and ambient temperature pathways, in which TEMs are also involved (Castillejo & Pelaz, 2008; Osnato *et al.*, 2012; Marín-González *et al.*, 2015), pointing to additional genetic pathway inter-communication within the flowering network.

MATERIALS AND METHODS

Plant material and growth conditions

Arabidopsis thaliana (L.) Heynh. Columbia-0 (Col-0) was used as the wild type for all the experiments. *tem1-1*, *tem2-2*, *tem1-1 tem2-2*, *RNAi-TEM1/2*, *35S::TEM1*, *35S::TEM2*, *pTEM1::GUS*, *35S::miR156*, *35S::MIM156, 35S::MIM172* and *pSPL9::rSPL9* plants have been previously described (Schwab *et al.*, 2005; Franco-Zorrilla *et al.*, 2007; Castillejo & Pelaz, 2008; Wang *et al.*, 2008; Todesco *et al.*, 2010; Osnato *et al.*, 2012). Seeds were stratified on wet filter paper in the dark at 4°C for 3-4 d and then sown on soil and grown in controlled environment chambers at 22°C under LDs (16 h light : 8 h dark) or SDs (8 h light : 16 h dark) at a light intensity of 80-90 μmol m^{-2} s^{-1}.

Phenotypic analyses

To determine the juvenile-to-adult transition we counted the rosette leaves without and with abaxial trichomes (juvenile and adult leaves, respectively). For flowering time experiments, the shoot apex was carefully checked for visible signs of flowering every two days. Flowering time was measured as the number of days from sowing to the appearance of the floral bud and as the total number of rosette and cauline leaves produced on the main stem. We used at least 8 plants per genotype in each experiment, although in most experiments we used 15-20 plants per genotype.

Analyses of miRNA and transcript levels

For miRNA analyses, total RNA was extracted from pools of at least 10 plants using the Real ARNzol Spin kit (+PVP; Durviz) or using Trizol (Ambion) following manufacturer's instructions. RNAs were treated with DNase I using the DNA-free kit (Ambion) and were precipitated with sodium acetate. Stem-loop reverse transcription followed by quantitative real time PCR (stem-loop RT-qPCR) and RNA blots were performed as previously described (Martin *et al.*, 2009). Primer and probe sequences are shown in Table S1.

For analyses of transcript levels by RT-qPCR, total RNA was extracted from pools of at least 10 plants with the Real ARNzol Spin kit (+PVP; Durviz), the PureLink RNA Mini kit (Ambion) or Trizol (Ambion), and was treated with DNase I using the DNA-free kit (Ambion). Reverse transcription was performed with 1-4 µg of RNA using Superscript III reverse transcriptase (Invitrogen), following manufacturer's instructions. qPCR was performed on a LightCycler® 480 Real-Time PCR System (Roche Diagnostics Ltd) with gene-specific primer pairs. The reactions, performed in triplicate in a volume of 14 µl, contained 0.2 µl of cDNA (except for *MIR172C*, see below), 1X Light Cycler 480 SYBR Green I Master mix (Roche), 0.3 µM forward primer and 0.3 µM reverse primer, and were incubated at 95°C for 10 min, followed by 45 cycles of 95°C for 15 s and 60°C for 1 min. The specificity of PCR was checked with dissociation curves and quantification was standardized to *UBIQUITIN10* (*UBQ10*) mRNA levels. Data from RT-qPCR were analyzed using the $2^{-\Delta\Delta C}{}_T$ method (Livak & Schmittgen, 2001). Primer sequences are listed in Table S1.

The analysis of *MIR172C* RNA levels was performed using TaqMan assays provided by Applied Biosystems (assay IDs: ARKA3K9 for *MIR172C* and At02163341_gH for *IPP2*). The qPCR reactions, performed in triplicate in a volume of 14 µl, contained 2 µl of cDNA, 1X TaqMan Multiplex Master mix (Applied Biosystems) and 1X TaqMan assay, and were incubated as indicated above. Quantification of *MIR172C* RNA was standardized to *IPP2* mRNA levels and data were analyzed using the $2^{-\Delta\Delta C}{}_T$ method (Livak & Schmittgen, 2001).

GUS staining

Histochemical analyses of GUS expression were performed as previously described (Blázquez *et al.*, 1997).

Identification of putative RAV binding sites

To find putative RAV binding sites, sequences of interest were searched for the pattern C[ACG][ACG]CAN(2,9)[ACT]NNCTG using Fuzznuc (http://emboss.bioinformatics.nl/cgi-bin/emboss/fuzznuc) or DNA Pattern Find (http://www.bioinformatics.org/sms2/dna_pattern.html).

Chromatin immunoprecipitation analyses

Chromatin immunoprecipitation (ChIP) experiments were performed using a modified version of a previously reported protocol (Matias-Hernandez *et al.*, 2010). Direct binding of TEM1 and TEM2 to the regulatory regions of putative targets was assayed using the *35S:TEM1-HA* and *35S:TEM2-HA* lines previously described (Castillejo & Pelaz, 2008). Wild-type plants were used as negative controls. The crosslinked DNA was immunoprecipitated with an anti-HA antibody (Sigma) and purified using Protein A-Agarose resin (Millipore). Enrichment of the target regions was determined by qPCR using different primer sets specific for putative direct targets, as listed in Table S1. The qPCR assay was conducted in triplicate using a SYBR Green Assay (SYBR Green Supermix, Roche) and was performed in a Roche LightCycler® 480 System. For the binding of TEM1 and TEM2 to the selected genomic regions, the affinity of the purified sample obtained in the *35S:TEM1-HA* and *35S:TEM2-HA* lines was compared with the affinity-purified sample obtained in the wild-type background, which was used as negative control. Fold enrichment, relative to wild-type input DNA immunoprecipitated with no antibody, was calculated using the $2^{-\Delta\Delta C}{}_{T}$ method (Livak & Schmittgen, 2001).

Transient expression assays

To generate the set of reporter vectors, different regions of *MIR172C* were cloned as SalI-PstI fragments in a modified pGreenII 0800-LUC vector carrying *p35S::LUC* (as reporter) and *p35S::REN* (as internal control to estimate the proportion of transformed protoplasts). Arabidopsis protoplasts were isolated from leaf-derived calli by digesting cell walls with Macerozyme R-10 and Cellulase (Yakult Pharmaceuticals). Protoplasts were transfected with different combinations of effector *p35S::TEM1* (Castillejo & Pelaz, 2008) and reporter constructs using PEG. After an overnight incubation in darkness at 24°C, transformed protoplasts were pelleted and resuspended in homogenization buffer for RNA extraction and DNase treatment with the Maxwell RSC Plant RNA kit (Promega), according to

manufacturer's protocol. Transcriptional repression activity of TEM1, based on the relative ratio of *Luciferase* (*LUC*) and *Renilla* (*REN*) mRNA abundance, was assessed by RT-qPCR. Primers used to generate the reporter vectors and for qPCR are listed in Table S1.

Genetic crosses

RNAi-TEM1/2 and *35S::MIM172* plants were crossed and the F_1 generation was allowed to self-pollinate. F_2 plants were selected based on resistance to kanamycin and Basta and were genotyped by checking resistance of the F_3 generation to kanamycin and Basta. F_3 homozygous plants were used for all the experiments.

Statistical analyses

Statistical analyses were performed with GraphPad Prism 6 or 7 software (GraphPad Software, Inc). Shapiro-Wilk normality tests were performed. For comparisons we used Student`s t test and ANOVA analyses, multiple comparisons were then corrected with Dunnett's or Tukey's test.

Data statement

Materials and data are available upon request to the corresponding authors.

Acknowledgements

We thank Detlef Weigel and Scott Poethig for seeds; Rossana Henriques for primers, discussion and critical reading of the manuscript; Mauricio Soto for advice with miRNA blots; Martí Bernardo for help with statistical analyses and data visualization; Laura Ossorio, Manel Giménez, Cristina Valdivieso and CRAG greenhouse staff for technical assistance; and Ángel Sánchez for pictures. This work was supported by the Spanish Ministry of Economy and Competitiveness/European Regional Development Fund (grants BFU2012-33746, BFU2015-64409-P and CSD2007-00036), the Catalonian Government (CERCA Programme, Consolidated Research Group no. 2014 SGR 1406 and Investigator Training Program PhD fellowship to A.E.A.-J.), and the Spanish Government (FPI fellowship to E.M.-G.). We acknowledge financial support from the Spanish Ministry of Economy and Competitiveness, through the "Severo Ochoa Programme for Centres of Excellence in R&D" 2016-2019 (SEV□2015□0533). A.E.A.-J. performed this work within the frame of a Ph.D. Program of the Universitat Autònoma de Barcelona.

Author contributions

P.S.-L., S.P. and E.M.-G. conceived and designed the experiments. A.E.A.-J., E.M.-G., L.M.-H., M.O. and P.S.-L. performed the experiments. A.E.A.-J., E.M.-G., L.M.-H., M.O., S.P. and P.S.-L. analyzed the data. P.S.-L. and S.P. wrote the manuscript, with input and comments from all other authors.

The authors declare that there is NO conflict of interest.

Supporting Information

Figure S1 Effect of TEMs, miR156, SPL9 and miR172 on the juvenile-to-adult transition.

Figure S2 Effect of TEMs, miR156, SPL9 and miR172 on flowering time.

Figure S3 Juvenile-to-adult transition of *RNAi-TEM1/2* plants.

Figure S4 Flowering time of *RNAi-TEM1/2* plants.

Figure S5 *TEM1* and *TEM2* mRNA levels in *35S::miR156* and *35S::MIM156* plants.

Figure S6 Diurnal oscillation of *SPL9* mRNA levels.

Figure S7 Mature miR156 levels in *tem1 tem2* and *35S::TEM1* plants.

Figure S8 Mature miR172 levels in *tem1 tem2* and *35S::TEM1* plants.

Figure S9 Silencing of transgenes by *tem1* and *35S::TEM1*.

Figure S10 *MIM172* RNA levels in *RNAi-TEM1/2 35S::MIM172* plants.

Figure S11 Juvenile-to-adult transition of *RNAi-TEM1/2 35S::MIM172* plants.

Figure S12 Flowering time of *RNAi-TEM1/2 35S::MIM172* plants.

Table S1 Primer sequences

Tables S2a-S2j Statistical analyses of data from Figure 1

Tables S3a-S3j Statistical analyses of data from Figure 2

Tables S4a-S4b Statistical analyses of data from Figure 3

Tables S5a-S5b Statistical analyses of data from Figure 4

Table S6 Putative RAV binding sites in *MIR172* genes

Tables S7a-S7b Statistical analyses of data from Figure 7

Tables S8a-S8b Statistical analyses of data from Figure 8

References

Amasino, R. (2010) Seasonal and developmental timing of flowering. *The Plant Journal* **61**, 1001-1013.

Andrés, F. and Coupland, G. (2012) The genetic basis of flowering responses to seasonal cues. *Nature Reviews Genetics*, **13**, 627-639.

Aukerman, M.J. and Sakai, H. (2003) Regulation of flowering time and floral organ identity by a microRNA and its *APETALA2*-like target genes. *The Plant Cell*, **15**, 2730-2741.

Blázquez, M.A., Soowal, L.N., Lee I. and Weigel, D. (1997) *LEAFY* expression and flower initiation in *Arabidopsis*. *Development*, **124**, 3835-3844.

Bouché, F., Lobet, G., Tocquin, P. and Périlleux, C. (2016) FLOR-ID: an interactive database of flowering-time gene networks in Arabidopsis thaliana. *Nucleic Acids Research*, **44**, D1167-D1171.

Castillejo, C. and Pelaz, S. (2008) The balance between CONSTANS and TEMPRANILLO activities determines FT expression to trigger flowering. *Current Biology*, **18**, 1338-1343.

Causier, B., Ashworth, M., Guo, W,. andDavies, B. (2012) The TOPLESS Interactome: A Framework for Gene Repression in Arabidopsis. *Plant Physiology*, **158**, 423-438.

Chen, X. (2004) A microRNA as a translational repressor of *APETALA2* in *Arabidopsis* flower development. *Science*, **303**, 2022-2025.

Cho, H.J., Kim, J.J., Lee, J.H., Kim, W., Jung, J.-H., Park, C.-M. and Ahn, .JH. (2012) SHORT VEGETATIVE PHASE (SVP) protein negatively regulates miR172 transcription via direct binding to the pri-miR172a promoter in Arabidopsis. *FEBS Letters*, **586**, 2332-2337.

Daxinger, L., Hunter, B., Sheikh, M., Jauvion, V., Gasciolli, V., Vaucheret, H., Matzke, M. and Furner, I. (2008) Unexpected silencing effects from T-DNA tags in Arabidopsis. *Trends In Plant Science*, **13**, 4-6.

Feng, C.-Z., Chen, Y., Wang, C., Kong, Y.-H., Wu, W.-H. and Chen, Y.-F. (2014) Arabidopsis RAV1 transcription factor, phosphorylated by SnRK2 kinases, regulates the expression of ABI3, ABI4, and ABI5 during seed germination and early seedling development. *The Plant Journal*, **80**, 654-668.

Franco-Zorrilla, J.M., Valli, A., Todesco, M., Mateos, I., Puga, M.I., Rubio-Somoza, I., Leyva, A., Weigel, D., García, J.A. and Paz-Ares, J. (2007) Target mimicry provides a new mechanism for regulation of microRNA activity. *Nature Genetics*, **39**, 1033-1037.

Galvão, V.C., Horrer, D., Küttner, F. and Schmid, M. (2012) Spatial control of flowering by DELLA proteins in *Arabidopsis thaliana*. *Development*, **139**, 4072-4082.

Gandikota, M., Birkenbihl, R.P., Hohmann, S., Cardon, G.H., Saedler, H. and Huijser, P. (2007) The miRNA156/157 recognition element in the 3' UTR of the Arabidopsis SBP box gene *SPL3* prevents early flowering by translational inhibition in seedlings. *The Plant Journal*, **49**, 683-693.

He, J., Xu, M., Willmann, M.R., McCormick, K., Hu, T., Yang, L., Starker, C.G., Voytas, D.F., Meyers, B.C. and Poethig, R.S. (2018) Threshold-dependent repression of SPL gene expression by miR156/miR157 controls vegetative phase change in *Arabidopsis thaliana*. *PLoS Genet*. **14**, e1007337.

Huijser, P. and Schmid, M. (2011) The control of developmental phase transitions in plants. *Development*, **138**, 4117-4129.

Hyun, Y., Richter, R., Vincent, C., Martinez-Gallegos, R., Porri, A. and Coupland, G. (2016) Multi-layered Regulation of SPL15 and Cooperation with SOC1 Integrate

Endogenous Flowering Pathways at the *Arabidopsis* Shoot Meristem. *Developmental Cell*, **37**, 254-266.

Ikeda, M. and Ohme-Takagi, M. (2009) A Novel Group of Transcriptional Repressors in Arabidopsis. *Plant and Cell Physiology*, **50**, 970-975.

Jung, J.-H., Ju, Y., Seo, P.J., Lee, J.-H. and Park, C.-M. (2012a) The SOC1-SPL module integrates photoperiod and gibberellic acid signals to control flowering time in Arabidopsis. *The Plant Journal*, **69**, 577–588.

Jung, J.-H., Seo, P., Kang, S. and Park, C.-M. (2011) miR172 signals are incorporated into the miR156 signaling pathway at the SPL3/4/5 genes in Arabidopsis developmental transitions. *Plant Molecular Biology*, **76**, 35-45.

Jung, J.-H., Seo, P.J., Ahn, J.H. and Park, C.-M. (2012b) *Arabidopsis* RNA-binding Protein FCA Regulates MicroRNA172 Processing in Thermosensory Flowering. *Journal of Biological Chemistry*, **287**, 16007-16016.

Jung, J.-H., Seo, Y.-H., Seo, P.J., Reyes, J.L., Yun, J., Chua, N.-H. and Park, C.-M. (2007) The *GIGANTEA*-regulated microRNA172 mediates photoperiodic flowering independent of *CONSTANS* in *Arabidopsis*. *The Plant Cell*, **19**, 2736-2748.

Kagaya, Y., Ohmiya, K. and Hattori, T. (1999) RAV1, a novel DNA-binding protein, binds to bipartite recognition sequence through two distinct DNA-binding domains uniquely found in higher plants. *Nucleic Acids Research*, **27**, 470-478.

Krogan, N.T., Hogan, K. and Long, J.A. (2012) APETALA2 negatively regulates multiple floral organ identity genes in *Arabidopsis* by recruiting the co-repressor TOPLESS and the histone deacetylase HDA19. *Development*, **139**,, 4180-4190.

Lee, H., Yoo, S.J., Lee, J.H., Kim, W., Yoo, S.K., Fitzgerald, H., Carrington, J.C. and Ahn, J.H. (2010) Genetic framework for flowering-time regulation by ambient temperature-responsive miRNAs in Arabidopsis. *Nucleic Acids Research*, **38**,, 3081-3093.

Livak, K.J. and Schmittgen, T.D. (2001) Analysis of relative gene expression data using real-time quantitative PCR and the $2^{-\Delta\Delta CT}$ Method. *Methods*, **25**, 402-408.

Long, J.A., Ohno, C., Smith, Z.R. and Meyerowitz, E.M. (2006) TOPLESS regulates apical embryonic fate in Arabidopsis. *Science*, **312**, 1520-1523.

Marín-González, E., Matías-Hernández, L., Aguilar-Jaramillo, A.E., Lee, J.H., Ahn, J.H., Suárez-López, P. and Pelaz, S. (2015) SHORT VEGETATIVE PHASE up-

regulates *TEMPRANILLO2* floral repressor at low ambient temperatures. *Plant Physiology*, **169**, 1214-1224.

Martin, A., Adam, H., Díaz-Mendoza, M., Żurczak, M., González-Schain, N.D. and Suárez-López, P. (2009) Graft-transmissible induction of potato tuberization by the microRNA *miR172*. *Development*, **136**, 2873-2881.

Mathieu, J., Yant, L.J., Mürdter, F., Küttner, F. and Schmid, M. (2009) Repression of Flowering by the miR172 Target SMZ. *PLoS Biology*, **7**, e1000148.

Matías-Hernández, L., Aguilar-Jaramillo, A.E., Marín-González, E., Suárez-López, P. and Pelaz, S. (2014) *RAV* genes: regulation of floral induction and beyond. *Annals of Botany*, **114**, 1459-1470.

Matías-Hernández, L., Aguilar-Jaramillo, A.E., Osnato, M., Weinstain, R., Shani, E., Suárez-López, P. and Pelaz, S. (2016) TEMPRANILLO reveals the mesophyll as crucial for epidermal trichome formation. *Plant Physiology*, **170**, 1624-1639.

Matias-Hernandez, L., Battaglia, R., Galbiati, F., Rubes, M., Eichenberger, C., Grossniklaus, U., Kater, M.M. and Colombo L. (2010) *VERDANDI* is a direct target of the MADS domain ovule identity complex and affects embryo sac differentiation in *Arabidopsis*. *The Plant Cell*, **22**, 1702-1715.

Osnato, M., Castillejo, C., Matías-Hernández, L. and Pelaz, S. (2012) *TEMPRANILLO* genes link photoperiod and gibberellin pathways to control flowering in *Arabidopsis*. *Nature Communications*, **3**, 808.

Park, J., Nguyen, K.T., Park, E., Jeon, J.-S. and Choi, G. (2013) DELLA Proteins and Their Interacting RING Finger Proteins Repress Gibberellin Responses by Binding to the Promoters of a Subset of Gibberellin-Responsive Genes in *Arabidopsis*. *The Plant Cell*, **25**, 927–943.

Picó, S., Ortiz-Marchena, M.I., Merini, W. and Calonje, M. (2015) Deciphering the role of Polycomb Repressive Complex 1 (PRC1) variants in regulating the acquisition of flowering competence in Arabidopsis. *Plant Physiology*, **168**, 1286-1297.

Poethig, R.S. (2009) Small RNAs and developmental timing in plants. *Current Opinion in Genetics & Development*, **19**, 374-378.

Rubio-Somoza, I. and Weigel, D. (2011) MicroRNA networks and developmental plasticity in plants. *Trends In Plant Science*, **16**, 258-264.

Schwab, R., Palatnik, J.F., Riester, M., Schommer, C., Schmid, M. and Weigel, D. (2005) Specific effects of microRNAs on the plant transcriptome. *Developmental Cell*, **8**, 517-527.

Schwarz, S., Grande, A.V., Bujdoso, N., Saedler, H. and Huijser, P. (2008) The microRNA regulated SBP-box genes *SPL9* and *SPL15* control shoot maturation in Arabidopsis. *Plant Molecular Biology*, **67**, 183-895.

Sgamma, T., Jackson, A., Muleo, R., Thomas, B. and Massiah, A. (2014) *TEMPRANILLO* is a regulator of juvenility in plants. *Scientific Reports*, **4**, 3704.

Tao, Z., Shen, L., Liu, C., Liu, L., Yan, Y. and Yu, H. (2012) Genome-wide identification of SOC1 and SVP targets during the floral transition in *Arabidopsis*. *The Plant Journal*, **70**, 549-561.

Telfer, A., Bollman, K.M. and Poethig, R.S. (1997) Phase change and the regulation of trichome distribution in *Arabidopsis thaliana*. *Development*, **124**, 645-654.

Todesco, M., Rubio-Somoza, I., Paz-Ares, J. and Weigel, D. (2010) A collection of target mimics for comprehensive analysis of microRNA function in *Arabidopsis thaliana*. *PLoS Genetics*, **6**, e1001031.

Wang, H. and Wang, H. (2015) The miR156/SPL Module, a Regulatory Hub and Versatile Toolbox, Gears up Crops for Enhanced Agronomic Traits. *Molecular Plant*, **8**, 677-688.

Wang, J.-W., Czech, B. and Weigel, D. (2009) miR156-Regulated SPL Transcription Factors Define an Endogenous Flowering Pathway in *Arabidopsis thaliana*. *Cell*, **138**, 738-749.

Wang, J.-W., Schwab, R., Czech, B., Mica, E. and Weigel, D. (2008) Dual Effects of miR156-Targeted *SPL* Genes and *CYP78A5/KLUH* on Plastochron Length and Organ Size in *Arabidopsis thaliana*. *The Plant Cell*, **20**, 1231-1243.

Wang, L., Zhou, C.-M., Mai, Y.-X., Li, L.-Z., Gao, J., Shang, G.-D.. Lian, H., Han, L., Zhang, T.-Q., Tang, H.-B., Ren, H., Wang, F.-X., Wu, L.-Y., Liu, X.-L., Wang, C.-S., Chen, E.-W., Zhang, X.-N., Liu, C. and Wang, J.-W. (2019) A spatiotemporally regulated transcriptional complex underlies heteroblastic development of leaf hairs in *Arabidopsis thaliana. EMBO J.*, **38**, **e100063**, DOI 10.15252/embj.2018100063.

Wang, L., Kim, J. and Somers, D.E. (2013) Transcriptional corepressor TOPLESS complexes with pseudoresponse regulator proteins and histone deacetylases to regulate circadian transcription. *Proceedings of the National Academy of Sciences of the United States of America*, **110**, 761-766.

Wu, G., Park, M.Y., Conway, S.R., Wang, J.-W., Weigel, D. and Poethig, R.S. (2009) The Sequential Action of miR156 and miR172 Regulates Developmental Timing in *Arabidopsis*. *Cell*, **138**, 750-759.

Wu, G. and Poethig, R.S. (2006) Temporal regulation of shoot development in Arabidopsis thaliana by miR156 and its target SPL3. *Development*, **133**, 3539-3547.

Yamaguchi, A., Wu, M.-F., Yang, L., Wu, G., Poethig, R.S. and Wagner, D. (2009) The MicroRNA-Regulated SBP-Box Transcription Factor SPL3 Is a Direct Upstream Activator of LEAFY, FRUITFULL, and APETALA1. *Developmental Cell*, **17**, 268-278.

Yant, L., Mathieu, J., Dinh, T.T., Ott, F., Lanz, C., Wollmann, H., Chen, X. and Schmid, M. (2010) Orchestration of the Floral Transition and Floral Development in *Arabidopsis* by the Bifunctional Transcription Factor APETALA2. *The Plant Cell*, **22**, 2156-2170.

Yu, S., Galvão, V.C., Zhang, Y.-C., Horrer, D., Zhang, T.-Q., Hao, Y.-H., Feng, Y.-Q., Wang, S., Markus, S. and Wang, J.-W. (2012) Gibberellin Regulates the Arabidopsis Floral Transition through miR156-Targeted SQUAMOSA PROMOTER BINDING–LIKE Transcription Factors. *The Plant Cell*, **24**, 3320-3332.

Figure legends

Figure 1. Effect of miR156, SPL9, miR172 and TEMs on the juvenile-to-adult transition in *Arabidopsis thaliana*. (a-j) Boxplots of the number of juvenile (a,c,e,g,i) and adult (b,d,f,h,j) leaves of the indicated genotypes grown under short day (SD, a-d) and long day (LD, e-j) conditions. The number of juvenile and adult leaves was determined by counting the rosette leaves without and with abaxial trichomes, respectively. The lines within the boxes represent the median and the whiskers represent the minimum and maximum values. Data represent the combination of two (a-d), three (e,f,i,j) or four (g,h) independent experiments, n=15-68. Asterisks indicate statistically significant differences relative to the WT (*, $P \leq 0.05$, **, $P \leq 0.01$, ***, $P \leq 0.001$, ****, $P \leq 0.0001$; ns, not significant), using one-way ANOVA followed by Dunnett's multiple comparison test (a-h) or using the Student's t test (i,j). Histograms and statistical analyses of these data are shown in Figure S1 and Tables S2a-S2j, respectively.

Figure 2. Effect of miR156, SPL9, miR172 and TEMs on flowering time in *Arabidopsis thaliana*. Boxplots of the number of total leaves (a,c,e,g,i) and days to flowering (b,d,f,h,j) of the indicated genotypes grown under short day (SD, a-d) and long day (LD, e-j) conditions. The lines within the boxes represent the median and the whiskers represent the minimum and maximum values. Data represent the combination of two (a-d,f), three (e,i,j) or four (g,h) independent experiments, n=15-68. Asterisks indicate statistically significant differences relative to the WT (*, $P \leq 0.05$, **, $P \leq 0.01$, ***, $P \leq 0.001$, ****, $P \leq 0.0001$; ns, not significant), using one-way ANOVA followed by Dunnett's multiple comparison test (a-h) or using the Student`s t test (i,j). Histograms and statistical analyses of these data are shown in Figure S2 and Tables S3a-S3j, respectively.

Figure 3. Juvenile-to-adult transition of *Arabidopsis thaliana RNAi-TEM1/2* plants. (a,b) Boxplots of the number of juvenile (a) and adult (b) leaves of WT and *RNAi-TEM1/2* plants grown under long day conditions. The number of juvenile and adult leaves was determined by counting the rosette leaves without and with abaxial trichomes, respectively. The lines within the boxes represent the median and the whiskers represent the minimum and maximum values. Data represent the combination of two independent experiments, n=52-59. Asterisks indicate statistically significant differences relative to the WT (***, $P \leq 0.001$), using the Student`s t test. Histograms and statistical analyses of these data are shown in Figure S3 and Tables S4a-S4b, respectively.

Figure 4. Flowering time of *Arabidopsis thaliana RNAi-TEM1/2* plants. (a,b) Boxplots of the number of total leaves (a) and days to flowering (b) of WT and *RNAi-TEM1/2* plants grown under long day conditions. The lines within the boxes represent the median and the whiskers represent the minimum and maximum values. Data represent the combination of two independent experiments, n=51-60. Asterisks indicate statistically significant differences relative to the WT (*, $P \leq 0.05$, ***, $P \leq 0.001$), using the Student`s t test. Histograms and statistical analyses of these data are shown in Figure S4 and Tables S5a-S5b, respectively. (c) WT and *RNAi-TEM1/2* plants grown under LD conditions for 21 days. Bars, 1 cm.

Figure 5. TEM1 and TEM2 affect *SPL* mRNA levels in *Arabidopsis thaliana*. (a-i) *SPL3* (a,d,g), *SPL9* (b,e,h) and *SPL15* (c,f,i) mRNA levels were determined by RT-qPCR in rosettes of 10-day-old *tem1 tem2* and *35S::TEM1* plants (a-c) or of plants of different ages (d-i) grown under long days (LDs), collected at ZT8 (a-f) and ZT18 (a-c,g-i). *UBQ10* was used

as normalization control and normalized levels in the wild type (a-c) or in the wild type at day 6 (d-i) were set to 1. Each symbol represents the mean of the combination of 2-5 independent experiments, n=2-5, and lines represent the standard error of the mean (SEM).

Figure 6. TEM1 and TEM2 regulate miR172 levels in *Arabidopsis thaliana*. (a-c) Mature miR172 levels in *tem1 tem2* (a,c) and *35S::TEM1* (b) plants were determined by RNA blot in rosettes of 10-day-old plants (a-b) or of plants of different ages (c) grown under long days (LDs), collected at ZT8 and ZT18. Hybridization to *U6* small nuclear RNA was used as a loading control. The numbers below each lane indicate the fold change relative to the miR172 level in the wild type at the corresponding ZT. (d) Binding of TEM1 to *MIR172C* chromatin by ChIP-qPCR. Chromatin from 11-day-old *35S::TEM1-H*A and *35S::TEM2-HA* plants grown under LDs was immunoprecipitated with an anti-HA antibody. Precipitated chromatin was used as template for qPCR using specific primers for a *MIR172C* fragment containing two putative RAV binding sites 109 and 186 nt downstream of the transcription start site. Data are presented as fold enrichment relative to WT input DNA immunoprecipitated without antibody. Error bars represent the standard deviation of three technical replicates. Three independent experiments gave similar results and one was chosen as representative. A schematic diagram of the *MIR172C* gene is shown above the graph. Black boxes indicate exons, an arrow indicates the transcription start site, inverted triangles indicate putative RAV binding sites and arrowheads indicate the fragment amplified by qPCR. (e) Repression of *MIR172C* expression by TEM1 in transient assays in Arabidopsis protoplasts. RT-qPCR was used to determine the relative ratio of Luciferase (LUC) and Renilla (REN) mRNA levels in protoplasts transformed with reporter constructs, with or without a *p35S::TEM1* effector construct. The reporter constructs carried the *LUC* gene under the control of a 35S promoter (*p35S::LUC*) or this promoter fused to fragments of the *MIR172C* gene containing or not containing putative RAV binding sites [*MIR172C(+)-p35S::LUC* and *MIR172C(-)-p35S::LUC*, respectively]. Data represent the combination of three independent experiments, n=3. (f) *MIR172C* (left), *MIR172A* (middle) and *MIR172B* (right) RNA levels in *tem1 tem2*, *RNAi-TEM1/2* and *35S::TEM1* plants were determined by RT-qPCR in rosettes of 19-day-old plants grown under LDs, collected at ZT8 and ZT18. *IPP2* (left) and *UBQ10* (middle and right) were used as normalization control and normalized levels in the wild type were set to 1. The symbols represent the mean of the combination of 3 independent experiments, n=3, and lines represent the SEM. Spaces in a) denote the removal of additional lanes bearing unrelated samples.

Figure 7. Juvenile-to-adult transition of *Arabidopsis thaliana RNAi-TEM1/2 35S::MIM172* plants. (a,b) Boxplots of the number of juvenile (a) and adult (b) leaves of WT, *RNAi-TEM1/2*, *35S::MIM172* and *RNAi-TEM1/2 35S::MIM172* plants grown under long day conditions. The number of juvenile and adult leaves was determined by counting the rosette leaves without and with abaxial trichomes, respectively. The lines within the boxes represent the median and the whiskers represent the minimum and maximum values. Data represent the combination of 3 independent experiments, n=59-60. Asterisks indicate statistically significant differences (**, $P \leq 0.01$, ****, $P \leq 0.0001$; ns, not significant), using one-way ANOVA followed by Tukey's multiple comparison test. Although the WT is shown as reference, only the relevant statistical analyses for the transgenic lines are shown. Histograms and statistical analyses of these data are shown in Figure S11 and Tables S7a-S7b, respectively.

Figure 8. Flowering time of *Arabidopsis thaliana RNAi-TEM1/2 35S::MIM172* plants. (a,b) Boxplots of the number of total leaves (a) and days to flowering (b) of WT, *RNAi-TEM1/2*, *35S::MIM172* and *RNAi-TEM1/2 35S::MIM172* plants grown under long day (LD) conditions. The lines within the boxes represent the median and the whiskers represent the minimum and maximum values. Data represent the combination of 3 independent experiments, n=60. Asterisks indicate statistically significant differences (***, $P \leq 0.001$; ns, not significant), using one-way ANOVA followed by Tukey's multiple comparison test. Although the WT is shown as reference, only the relevant statistical analyses for the transgenic lines are shown. Histograms and statistical analyses of these data are shown in Figure S12 and Tables S8a-S8b, respectively. (c) WT, *RNAi-TEM1/2*, *35S::MIM172* and *RNAi-TEM1/2 35S::MIM172* plants grown under LD conditions for 23 days. Bars, 1 cm.

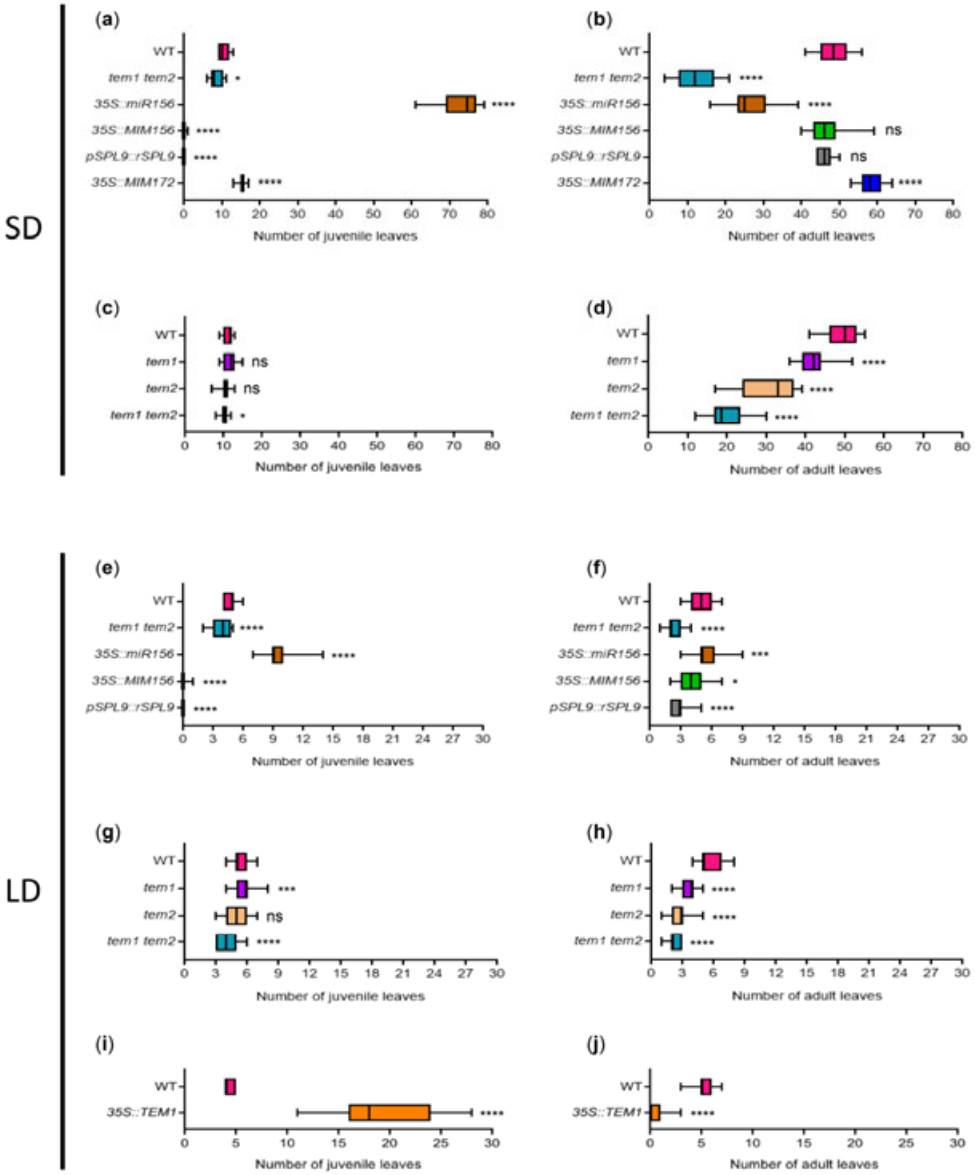

Figure 1

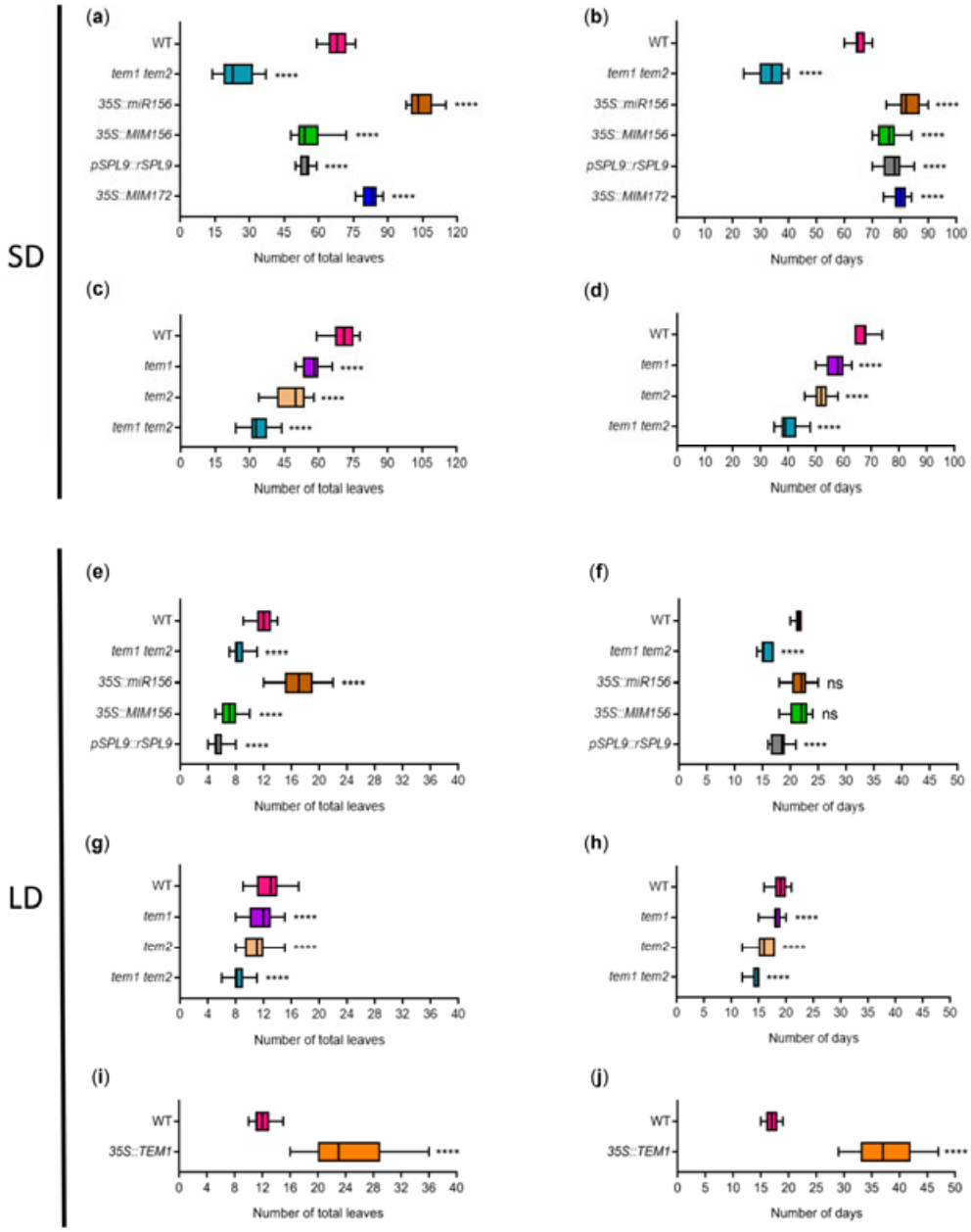

Figure 2

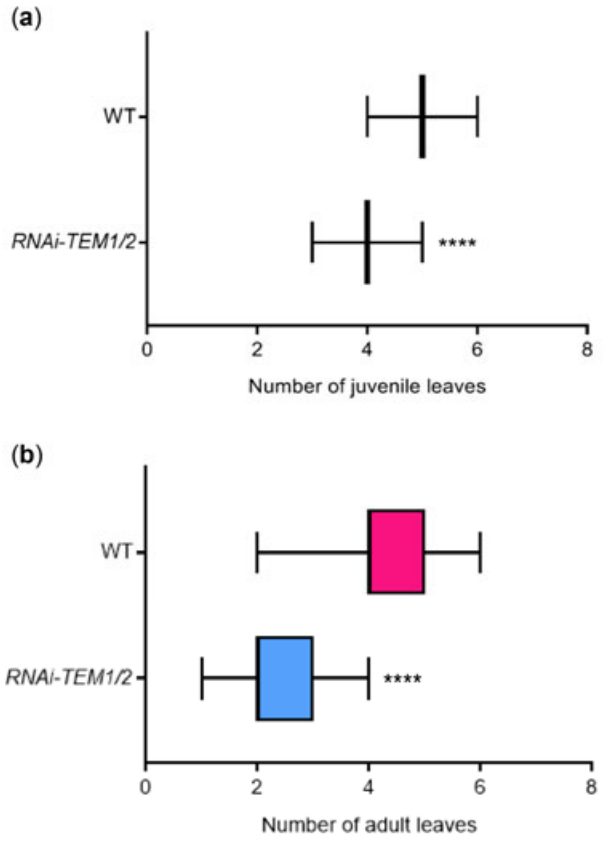

Figure 3

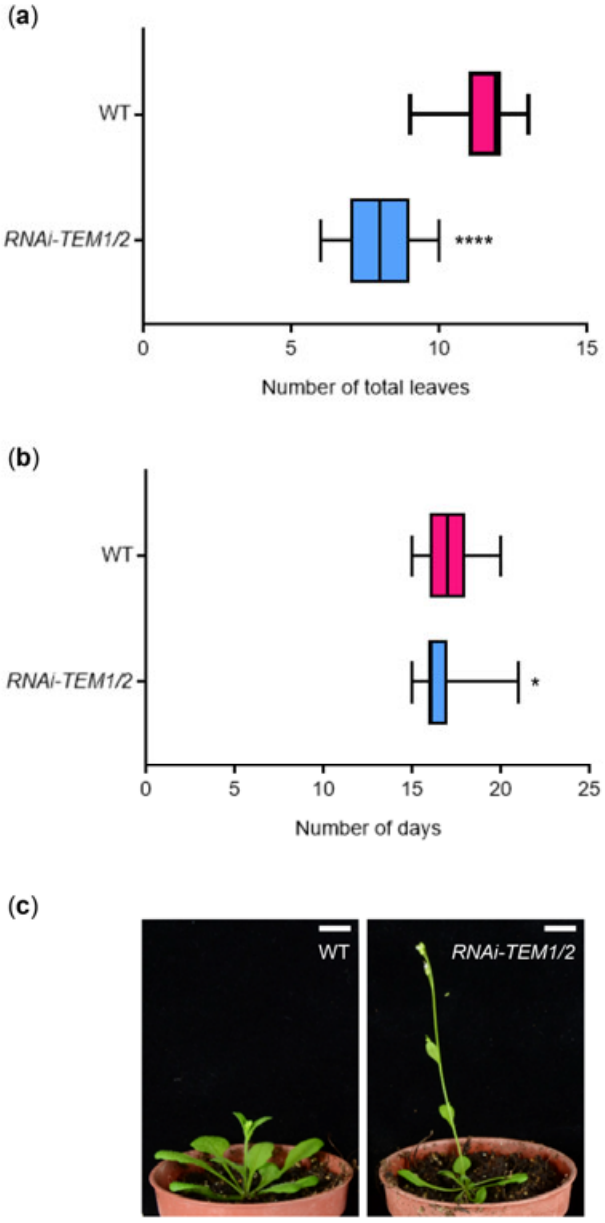

Figure 4

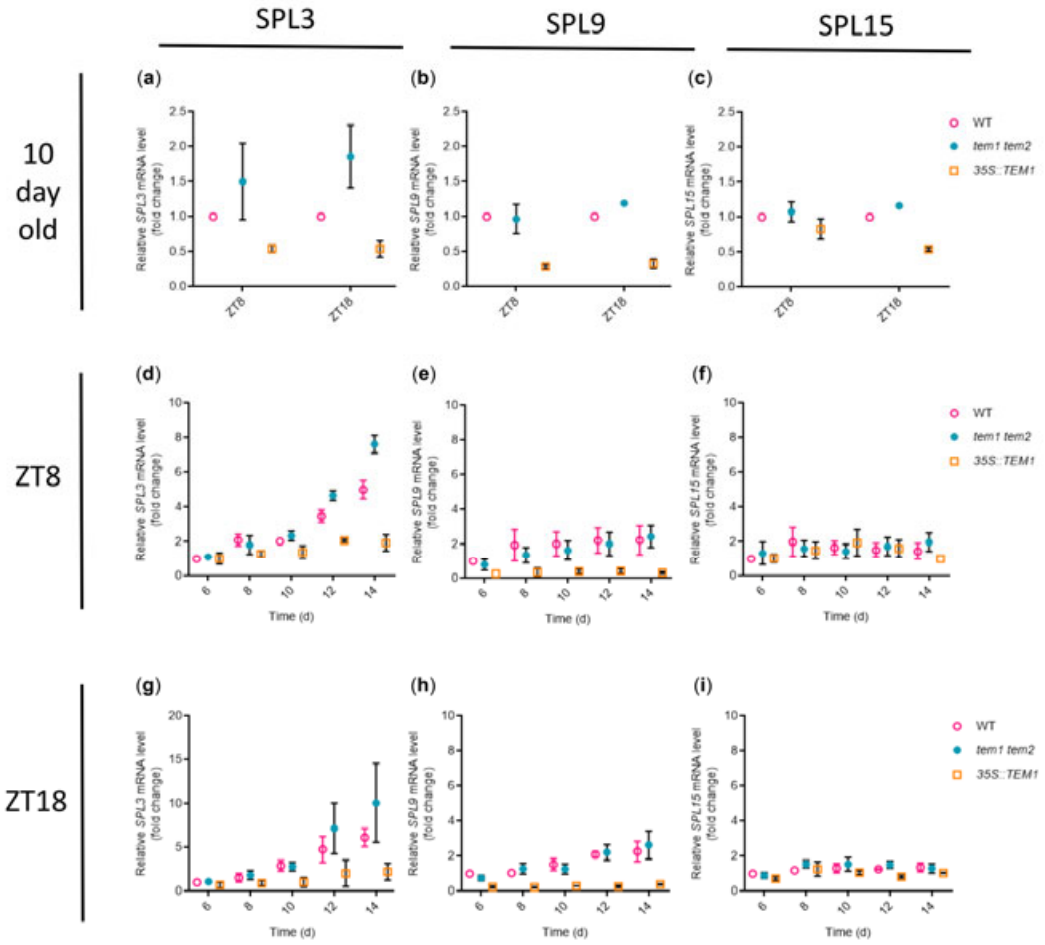

Figure 5

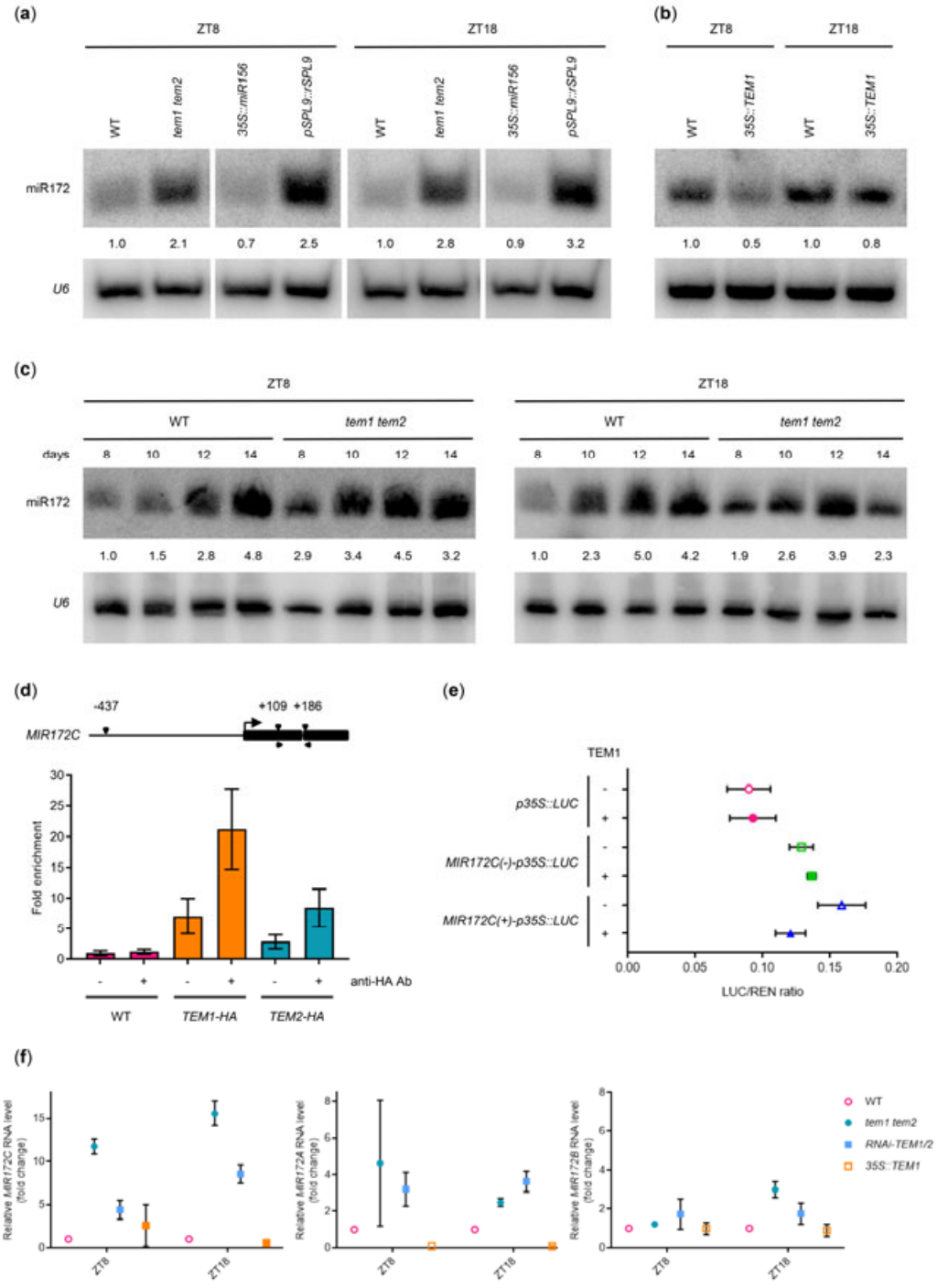

Figure 6

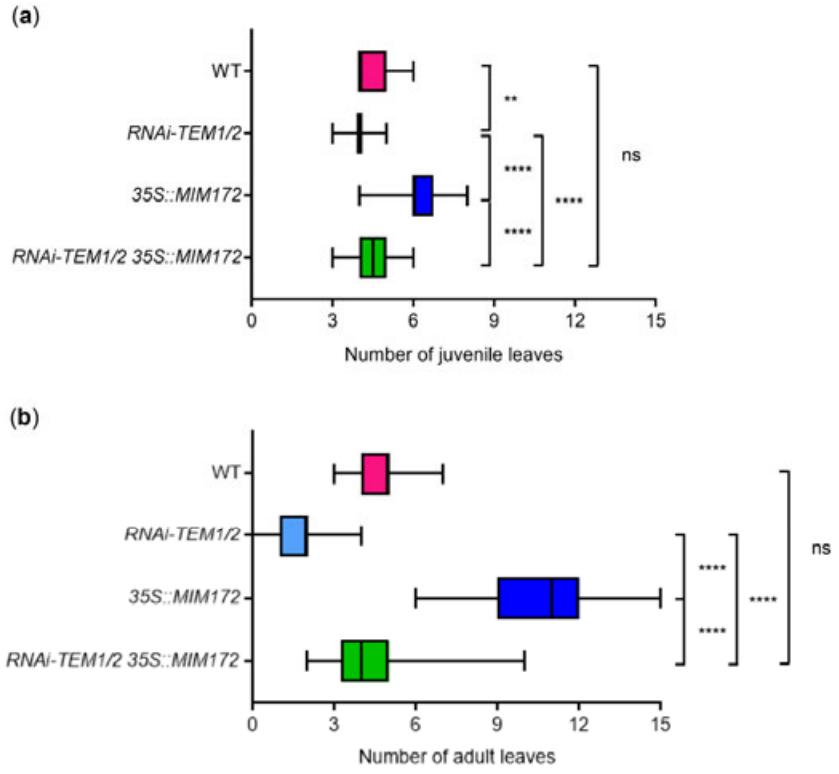

Figure 7

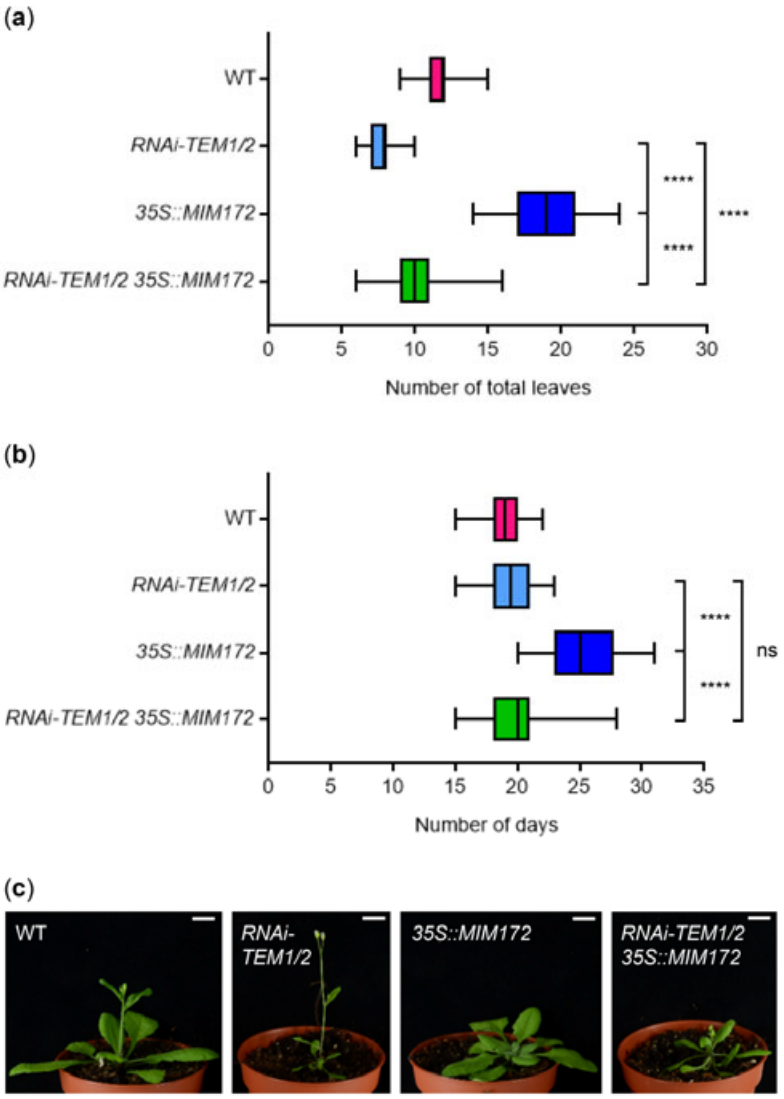

Figure 8